

Quantum circuits for digital quantum simulation of nonlocal electron-phonon coupling

Vladimir M. Stojanović*

Institut für Angewandte Physik, Technical University of Darmstadt, D-64289 Darmstadt, Germany

(Dated: October 11, 2024)

Motivated by the compelling need to understand the nonequilibrium dynamics of small-polaron formation following an electron-phonon interaction quench, in this work we propose a digital quantum simulator of a one-dimensional lattice model describing an itinerant fermionic excitation (e.g. an electron) nonlocally coupled to zero-dimensional bosons (e.g. Einstein-type phonons). Quantum circuits implementing the dynamics of this model, which includes Peierls- and breathing-mode-type excitation-boson interactions, are designed here, their complexity scaling linearly with the system size. A circuit that generates the natural initial (pre-quench) state of this system – a bare-excitation Bloch state, equivalent to a W state of a qubit register – is also presented. To facilitate comparisons with the proposed simulator, once experimentally realized, the system dynamics are also evaluated numerically and characterized through the Loschmidt echo and various correlation functions.

Inspired by Feynman’s pioneering idea that a quantum system could efficiently be simulated using a device that is also governed by quantum-mechanical laws [1], the field of quantum simulation is at the current frontier of physics research [2]. While analog quantum simulators of many-body systems were intensively studied already a decade ago [3], the ongoing spate of activity in the realm of *digital quantum simulation* (DQS) [3–5] is mainly motivated by the considerable progress in the development of quantum hardware [6] achieved in recent years [7–9]. In particular, owing to the relatively modest resources required for their execution, quantum algorithms for simulating fermionic systems have as yet been most extensively studied [10–21]. On the other hand, digital simulators of bosonic (or fermion-boson) systems have heretofore received much less attention [22–27].

Electron-phonon (e-ph) coupling is pervasive in solid-state systems [28], being arguably the most important interaction mechanism that involves both bosons and fermions. In particular, one common physical situation in narrow-band semiconductors and insulators entails an itinerant excitation (electron, hole) experiencing a short-ranged, nonpolar interaction with the host-crystal lattice vibrations. Such phenomena are typically described within the framework of the Holstein model [29, 30], the strong-coupling regime of which captures the formation of a heavily-dressed quasiparticle known as *small polaron* (SP) [31]. While this model only takes into account local coupling of the excitation density and an Einstein-phonon displacement, the need to describe complex electronic materials [28] has prompted investigations of non-local e-ph interactions [32–35]. This line of research has even led to the discovery of sharp SP ground-state transitions of level-crossing type [36–38] in certain models with strongly momentum-dependent e-ph interactions [39].

While several analog simulators of coupled e-ph models were proposed in the past [38, 40–44], only the Holstein model was addressed in the DQS context [22, 23, 45]. Aiming to change this state of affairs, this paper presents DQS of a one-dimensional (1D) lattice model describ-

ing an itinerant fermionic excitation (e.g. an electron) coupled to dispersionless bosons (e.g. Einstein-type phonons) through breathing-mode- [46] and Peierls-type [36] interactions. Quantum circuits emulating these short-ranged yet nonlocal interactions are presented here, with their complexity scaling linearly with the system size.

In contrast to the existing works on DQS of coupled e-ph models [22, 23], which solely discuss the already well-understood ground-state properties of Holstein-type SPs [30], the present work is chiefly concerned with the nonequilibrium SP physics; the ground-state properties will also be discussed, but mainly for benchmarking purposes. The current understanding of the latter, especially of the complex process of SP formation following an e-ph interaction quench (i.e., a sudden switching-on of the e-ph coupling) is by no means satisfactory [47, 48]. In principle, recent advances in ultrafast time-resolved spectroscopies [49] opened the possibilities to investigate such processes experimentally. Yet, many important questions remain unanswered due to the impossibility of fully separating the effects of e-ph coupling from the other interaction mechanisms in solid-state systems. Thus, the incentive to explore the quench dynamics of SP formation within a well-controlled DQS setting – as attempted in this paper – is compelling.

Model Hamiltonian.– The model under consideration envisions a spinless-fermion excitation with the hopping amplitude t_e on a 1D lattice where each site hosts dispersionless bosons (or, equivalently, a zero-dimensional harmonic oscillator). The noninteracting part of the system Hamiltonian \hat{H}_{sys} consists of the excitation kinetic-energy- and free-boson terms (hereafter $\hbar = 1$):

$$\hat{H}_0 = -t_e \sum_n (\hat{c}_{n+1}^\dagger \hat{c}_n + \text{H.c.}) + \omega_b \sum_n \hat{b}_n^\dagger \hat{b}_n. \quad (1)$$

Here \hat{c}_n^\dagger (\hat{c}_n) creates (destroys) a spinless-fermion excitation at site n ($n = 1, \dots, N$) and \hat{b}_n^\dagger (\hat{b}_n) a boson with frequency ω_b at the same site. The interacting (e-b) part

of \hat{H}_{sys} is given by $\hat{H}_{\text{e-b}} = \hat{H}_{\text{P}} + \hat{H}_{\text{B}}$, where

$$\begin{aligned}\hat{H}_{\text{P}} &= \alpha_{\text{P}} \sum_n (\hat{c}_{n+1}^\dagger \hat{c}_n + \text{H.c.}) (\hat{x}_{n+1} - \hat{x}_n), \\ \hat{H}_{\text{B}} &= \alpha_{\text{B}} \sum_n \hat{c}_n^\dagger \hat{c}_n (\hat{x}_{n-1} - \hat{x}_{n+1}),\end{aligned}\quad (2)$$

and $\hat{x}_n \equiv \xi_0 (\hat{b}_n^\dagger + \hat{b}_n)$ is the displacement operator of the oscillator at site n , with ξ_0 being its zero-point length. \hat{H}_{P} accounts for the lowest-order dependence of the effective excitation-hopping amplitude between two adjacent lattice sites on the respective displacements (Peierls-type coupling) [33, 36], while \hat{H}_{B} describes the anti-symmetric coupling of the excitation density on a given site with the displacements at the two adjacent sites (breathing-mode-type coupling) [46]. As a manifestation of the discrete translational symmetry, the Hamiltonian $\hat{H}_{\text{sys}} = \hat{H}_0 + \hat{H}_{\text{P}} + \hat{H}_{\text{B}}$ commutes with the total quasimomentum operator $\hat{K} = \sum_k k \hat{c}_k^\dagger \hat{c}_k + \sum_q q \hat{b}_q^\dagger \hat{b}_q$, where \hat{c}_k^\dagger and \hat{b}_q^\dagger are the respective momentum-space counterparts of the operators \hat{c}_n^\dagger and \hat{b}_n^\dagger .

Quench dynamics from DQS.— The system dynamics following an e-b interaction quench at $t = 0$ are considered here within the DQS framework. Use will be made of the first-order Trotter-Suzuki-type decomposition [50, 51]. For a Hamiltonian $\hat{H} = \sum_l \hat{H}_l$ the latter approximates $\exp(-i\hat{H}t)$ by $(\prod_l e^{-i\hat{H}_l t/n_s})^{n_s}$, with the corresponding error being upper bounded by $\mathcal{O}(Nt^2/n_s)$, where N is the number of qubits and n_s that of time steps [4]. To this end, the time-evolution operator $\hat{U}_{\text{sys}} \equiv \exp(-i\hat{H}_{\text{sys}}t)$ of the system at hand is represented through quantum circuits that emulate the dynamics inherent to the Hamiltonians \hat{H}_0 , \hat{H}_{P} , and \hat{H}_{B} .

In the DQS context one switches from spinless-fermion to qubit degrees of freedom via the Jordan-Wigner transformation (JWT) [52], which assumes an ordering of the qubits and maps the fermionic operators \hat{c}_n^\dagger and \hat{c}_n to the (qubit) Pauli operators X_n, Y_n, Z_n according to $2\hat{c}_n^\dagger \rightarrow (X_n - iY_n)Z_1 \dots Z_{n-1}$ and $2\hat{c}_n \rightarrow (X_n + iY_n)Z_1 \dots Z_{n-1}$. The state $|1_n\rangle$ of qubit n corresponds to a spinless-fermion occupying the lattice site n , while $|0_n\rangle$ represents an unoccupied site n .

The natural initial (pre-quench) state $|\psi_{t=0}\rangle$ of the system at hand is the ground state of the Hamiltonian \hat{H}_0 , i.e. the bare-excitation Bloch state at zero quasimomentum $|\Psi_{k=0}\rangle \equiv c_{k=0}^\dagger |0\rangle_{\text{e}} \otimes |0\rangle_{\text{b}}$. Using the JWT it is straightforward to establish that $|\Psi_{k=0}\rangle = |W_N\rangle \otimes |0\rangle_{\text{b}}$, where $|W_N\rangle$ is an N -qubit W state [53, 54]:

$$|W_N\rangle = N^{-1/2} \sum_{n=1}^N |0 \dots 1_n \dots 0\rangle. \quad (3)$$

W-state generating circuit.— In what follows, a quantum circuit is proposed that generates the state in Eq. (3) when acting on an N -qubit register. The circuit constitutes a digital counterpart of an analog scheme in

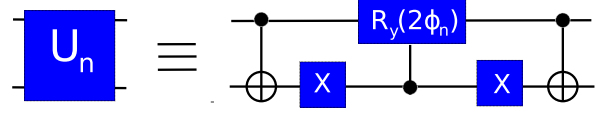


FIG. 1: (Color online) Quantum-circuit representation of the unitaries $U_n(\phi_n)$, where $R_y(2\phi_n) \equiv \exp(-i\phi_n Y)$ stands for a y -axis rotation by an angle of $2\phi_n$ ($n = 1, \dots, N$).

which W states are generated through sequential entanglement of an auxiliary qubit 0 with each of the qubits $1, 2, \dots, N$ [55]; it is assumed that the whole $(N+1)$ -qubit system is initialized in the state $|0_0\rangle \otimes |0\rangle^{\otimes N}$. To create entanglement between qubits 0 and n ($n = 1, \dots, N$), one considers the following parameterized unitary operation:

$$\begin{aligned}U_n(\phi_n) &= |0_0 1_n\rangle\langle 0_0 1_n| + |1_0 0_n\rangle\langle 1_0 0_n| \\ &+ \cos \phi_n (|0_0 0_n\rangle\langle 0_0 0_n| + |1_0 1_n\rangle\langle 1_0 1_n|) \\ &+ \sin \phi_n (|1_0 1_n\rangle\langle 0_0 0_n| - |0_0 0_n\rangle\langle 1_0 1_n|).\end{aligned}\quad (4)$$

For each choice of ϕ_n , U_n generates a superposition of $|0_0 0_n\rangle$ and $|1_0 1_n\rangle$, acting trivially on the remaining $N - 1$ qubits. The circuit representation of U_n , which entails two single-qubit (NOT) gates and three two-qubit gates [one controlled- y rotation- and two controlled-NOT (CNOT) gates], is shown in Fig. 1.

The chosen W -state preparation scheme envisions applying $U_n(\phi_n)$ for $n = 1, \dots, N$ sequentially on the initial state. The first step in this scheme gives rise to $U_1(\phi_1)|0_0 0_1\rangle = \cos \phi_1 |0_0 0_1\rangle + \sin \phi_1 |1_0 1_1\rangle$. While subsequent application of the unitaries $U_n(\phi_n)$ for $n \geq 2$ engenders a broad family of entangled states, it is straightforward to show that for one special choice of ϕ_n one obtains the final state $|1\rangle \otimes |W_N\rangle$, where $|W_N\rangle$ is given by Eq. (3). This choice is described by the conditions $\prod_{n=1}^N \cos \phi_n = 0$ and $\cos \phi_n |\sin \phi_{n+1}| = |\sin \phi_n|$, which yield the solution $\sin \phi_n = (N + 1 - n)^{-1/2}$. The circuit generating the desired W state in a 1D qubit array using a sequence of alternating U_n and SWAP operations is illustrated in Fig. 2.

Based on the circuit representation of U_n (cf. Fig. 1) and the fact that a SWAP operation can be realized using three CNOT gates [56], one concludes that $\mathcal{O}(N)$ gates are required for generating the state $|W_N\rangle$ using this scheme.

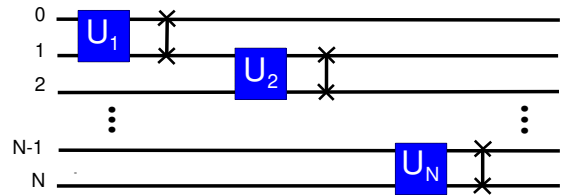


FIG. 2: (Color online) Quantum circuit generating the initial W -type state of the system when acting on a $(N + 1)$ -qubit register initialized in the state $|0\rangle \otimes |0\rangle^{\otimes N}$.

Boson-state encoding.— One of the prerequisites for the envisioned DQS is the capability to encode bosonic states on qubits. To this end, use will be made of a recently proposed method based on the idea of controlled truncation of bosonic Hilbert spaces [23], whose rigorous foundation rests on a generalized Nyquist-Shannon sampling theorem [24]. In the case of zero-dimensional oscillators, the number n_q of required qubits per lattice site in this approach scales as $\log[\log(1/\epsilon)]$, where ϵ is the desired accuracy [23]. In keeping with Ref. [23], in what follows the states $|x_n\rangle$ of the oscillator on site n are encoded in such a way that the index r of each qubit within the register of n_q qubits is defined by the binary representation $x_n = \sum_{r=0}^{n_q-1} x_n^r 2^r$ of x_n ($x_n^r = 0, 1$). Finally, the dimensionless ($\xi_0 \rightarrow 1$) coordinate and momentum operators in the 2^{n_q} -dimensional truncated Hilbert space of the oscillator n will be denoted by \tilde{x}_n and \tilde{p}_n .

In particular, quantum circuits pertaining to the coordinate part of the free boson Hamiltonian, i.e. the time-evolution operator $e^{-i\theta\tilde{x}_n^2}$, were proposed in Ref. [23]. They involve controlled phase-shift gates $T(\theta_r) \equiv \text{diag}(1, e^{-i\theta_r})$ acting on each qubit in the boson register, with $\theta_r \equiv 2^r\theta$. On the other hand, the realization of circuits corresponding to $e^{-i\theta\tilde{p}_n^2}$ requires one to first implement a quantum Fourier transform from $\{|p_n\rangle, n = 1, \dots, N\}$ to $\{|x_n\rangle, n = 1, \dots, N\}$, then the same type of circuits as for $e^{-i\theta\tilde{x}_n^2}$, and, finally, carry out the inverse quantum Fourier transform [5].

Circuits for $e^{-i\theta\hat{H}_B}$ and $e^{-i\theta\hat{H}_P}$.— Quantum circuits [56] representing the interaction terms \hat{H}_B and \hat{H}_P are presented in the following. They partially inherit the structure of purely fermionic circuits [11, 13, 15] which are expressed in terms of the Hadamard gates H_n , the z -rotation gates $R_{z,n}(\theta) \equiv \exp(-i\theta Z_n/2) =$

$\text{diag}(e^{i\theta/2}, e^{-i\theta/2})$, and the phase-shift gates $T_n(\theta)$ ($n = 1, \dots, N$). The boson (oscillator) states define the attendant rotation- and phase-shift angles.

To find the circuit representation of the time-evolution operator corresponding to the Hamiltonian \hat{H}_B one makes use of the fact that the JWT maps $\hat{c}_n^\dagger \hat{c}_n$ into $(1 - Z_n)/2 \dots$ where $\theta_{n-1, n+1} \equiv (x_{n-1} - x_{n+1})\theta$. The resulting circuit implementing $e^{-i\theta\hat{H}_B}$ is shown in Fig. 3(a).

Recalling that JWT transforms $\hat{c}_{n+1}^\dagger \hat{c}_n + \hat{c}_n^\dagger \hat{c}_{n+1}$ into $(X_n X_{n+1} + Y_n Y_{n+1})/2$ and using a Trotter-type decomposition, the time-evolution operator corresponding to the Hamiltonian \hat{H}_P can be approximated as $e^{-i\theta\hat{H}_P} \approx U_Y(\theta)U_X(\theta)$, where

$$\begin{aligned} U_X(\theta) &\equiv e^{-i\frac{\theta}{2}X_n X_{n+1}(\tilde{x}_{n+1} - \tilde{x}_n)}, \\ U_Y(\theta) &\equiv e^{-i\frac{\theta}{2}Y_n Y_{n+1}(\tilde{x}_{n+1} - \tilde{x}_n)}. \end{aligned} \quad (5)$$

By making use of the basis-change transformations $H_n Z_n H_n = X_n$ and $R_{x,n}(-\pi/2)Z_n R_{x,n}(\pi/2) = Y_n$ and the fact that for an arbitrary unitary U and an analytic operator function $f(A)$ it holds that $Uf(A)U^{-1} = f(UAU^{-1})$, one straightforwardly demonstrates that

$$\begin{aligned} U_X(\theta) &= H_n H_{n+1} e^{-i\frac{\theta}{2}Z_n Z_{n+1}(\tilde{x}_{n+1} - \tilde{x}_n)} H_n H_{n+1}, \\ U_Y(\theta) &= R_{x,n}(-\pi/2)R_{x,n+1}(-\pi/2)e^{-i\frac{\theta}{2}Z_n Z_{n+1}(\tilde{x}_{n+1} - \tilde{x}_n)} \\ &\quad \times R_{x,n}(\pi/2)R_{x,n+1}(\pi/2). \end{aligned} \quad (6)$$

Using the standard circuit representation of the time-evolution operators of the type $e^{-i\frac{\theta}{2}Z_n Z_{n+1}}$ with one $R_z(\theta)$ and two CNOT gates [13], the operator $e^{-i\frac{\theta}{2}Z_n Z_{n+1}(\tilde{x}_{n+1} - \tilde{x}_n)}$ can be represented in an analogous fashion, with the z -rotation angle $\theta_{n+1, n} \equiv (x_{n+1} - x_n)\theta$ determined by the states of the oscillators n and $n + 1$.

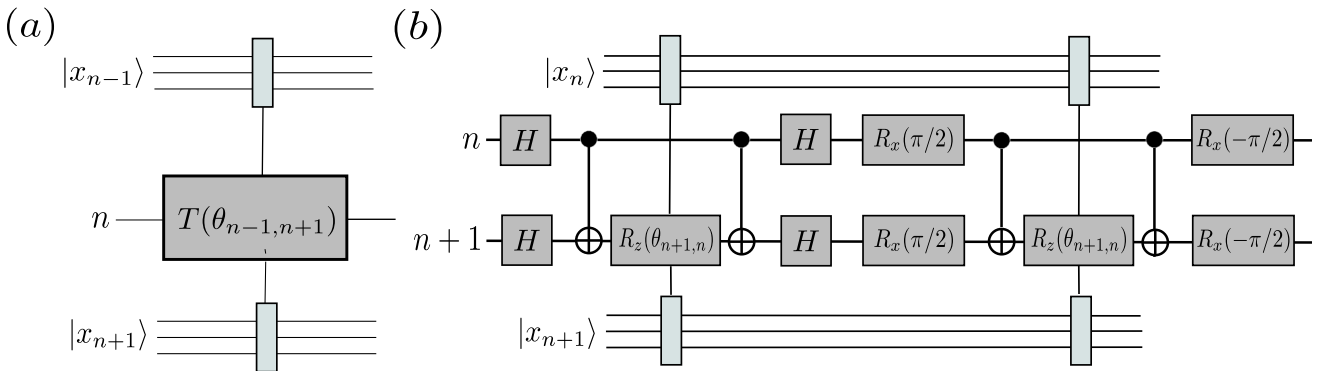


FIG. 3: (Color online) Quantum circuits corresponding to (a) breathing-mode type coupling (\hat{H}_B), and (b) Peierls-type coupling (\hat{H}_P). The relevant z -rotation angles are defined as $\theta_{n-1, n+1} \equiv (x_{n-1} - x_{n+1})\theta$ and $\theta_{n+1, n} \equiv (x_{n+1} - x_n)\theta$.

Based on Eqs. (5) and (6), the resulting circuit implementing $e^{-i\theta\hat{H}_P}$ has the form illustrated in Fig. 3(b).

Ground-state evaluation.— To benchmark the proposed digital simulator we extract the ground-state properties of the system using quantum phase estimation (QPE) algorithm [57]. These properties can be computed classically – to requisite precision – using Lanczos-type diagonalization of the total system Hamiltonian.

The momentum-space form of H_{e-b} reads

$$\hat{H}_{e-b} = N^{-1/2} \sum_{k,q} \gamma_{e-b}(k,q) \hat{c}_{k+q}^\dagger \hat{c}_k (\hat{b}_{-q}^\dagger + \hat{b}_q), \quad (7)$$

where the e-b vertex function is given by $\gamma_{e-b}(k,q) = 2i\omega_b \{g_B \sin q + g_P [\sin k - \sin(k+q)]\}$, where $g_B \equiv \alpha_B \xi_0$ and $g_P \equiv \alpha_P \xi_0$ are the respective dimensionless coupling strengths. The most interesting ground-state aspect of such couplings is the possible occurrence of sharp transitions, i.e. a nonanalyticity of the ground state energy at a critical coupling strength. It is already known that a Hamiltonian with Peierls- and breathing-mode-type couplings shows such sharp transition. Given that the presence of Peierls-type coupling alone suffices for obtaining a sharp transition – while breathing-mode coupling does not have this property (a consequence of the fact that its vertex function depends only on q) – it makes sense to use the effective Peierls-coupling strength λ_P and the ratio $\zeta \equiv g_B/g_P$ as the two dimensionless parameters characterizing e-ph coupling in the system at hand. Recalling that for the most general e-b coupling described by the vertex function $\gamma_{e-b}(k,q)$ [cf. Eq. (7)] the corresponding effective e-b coupling strength is given by $\langle |\gamma_{e-b}(k,q)|^2 \rangle_{BZ}$, where $\langle \dots \rangle_{BZ}$ stands for the Brillouin zone average, in the special case of Peierls coupling one straightforwardly obtains $\lambda_P = 2 g_P^2 \omega_b / t_e$.

Dynamics following an interaction quench.— The nonequilibrium dynamics of a quantum system after an interaction quench at $t = 0$ are, generally speaking, best characterized by the Loschmidt amplitude [58]

$$\mathcal{G}(t) = \langle \psi_{t=0} | e^{-i\hat{H}_{sys}t} | \psi_{t=0} \rangle, \quad (8)$$

i.e. the overlap of the initial state $|\psi_{t=0}\rangle$ and its time-evolved counterpart $e^{-i\hat{H}_{sys}t} |\psi_{t=0}\rangle$ at time t . This quantity is closely related – more precisely, up to a Fourier transform to the frequency domain – to an important dynamical response function, namely the momentum-frequency resolved spectral function. The squared modulus of $\mathcal{G}(t)$ – i.e. the survival probability $\mathcal{L}(t) \equiv |\mathcal{G}(t)|^2$ of the initial state at time t – is a special case of the quantity known as the Loschmidt echo [59]. Because the initial state $|\psi_{t=0}\rangle$ (in the problem at hand a bare-excitation Bloch state) is, generally speaking, not an eigenstate of the system Hamiltonian after the quench – but rather a linear combination of its multiple eigenstates – $\mathcal{L}(t)$ usually shows a complex oscillatory dependence on time t , indicating the presence of dynamical recurrences.

For the sake of comparison with the proposed simulator, once implemented on a NISQ hardware, the system dynamics can be computed classically. Because

$[\hat{H}_{sys}, \hat{K}_{tot}] = 0$, the system evolves within the eigensubspace of \hat{H}_{sys} that corresponds to the eigenvalue $K = 0$ of \hat{K}_{tot} . Its state $|\psi(t)\rangle$ at time t is computed here for $N = 9$ qubits by combining Lanczos-type exact diagonalization [60] of \hat{H}_{sys} in a symmetry-adapted basis of the truncated Hilbert space of the system and an expansion of \hat{U}_{sys} into a finite series of Chebyshev polynomials of the first kind [61, 62].

Conclusions and Outlook.— Aiming to provide a reliable testbed for exploring the nonequilibrium dynamics of SP formation following an e-ph interaction quench, this paper presented a DQS of nonlocal e-ph interactions. Quantum circuits emulating e-ph interactions of Peierls- and breathing-mode types, along with a circuit generating the initial W -type state of the system, form the backbone of the envisioned simulator. To enable future comparisons with this simulator – once practically realized – both the ground-state properties of the considered model and its dynamics were computed classically in a numerically-exact fashion.

The DQS proposed here will facilitate advances in the general understanding of the nonequilibrium properties of polaronic quasiparticles [63]. More generally speaking, it strongly reinvigorates the idea of using DQS to investigate the quench dynamics of quantum many-body systems [64], a research approach which is still in the stage of infancy [65] despite the developments of quantum hardware.

The proposed DQS complements the existing simulators of interacting fermions. Hybrid simulators, capable of emulating both strong electron correlations and e-ph interactions, may become indispensable in investigating complex electronic materials. A case in point are cuprates, the parent compounds of high-temperature superconductors, where the two e-ph coupling mechanisms addressed here play important roles [34]. While the currently available quantum-computing setups [7–9] (systems containing from 50 to a few hundred qubits) belong to the realm of noisy intermediate-scale quantum technology [6], their further development (in terms of qubit count, quality, and connectivity), along with the optimization of DQS algorithms [14, 66] of the kind proposed here using machine-learning-based methods [67, 68], may allow exploration of complex many-body phenomena.

This research was supported by the Deutsche Forschungsgemeinschaft (DFG) – SFB 1119 – 236615297.

* Electronic address: vladimir.stojanovic@physik.tu-darmstadt.de

- [1] R. P. Feynman, Int. J. Theor. Phys. **21**, 467 (1982).
- [2] For an up-to-date review, see E. Altman *et al.*, PRX Quantum **2**, 017003 (2021).
- [3] I. M. Georgescu, S. Ashhab, and F. Nori, Rev. Mod. Phys. **86**, 153 (2014).
- [4] S. Lloyd, Science **273**, 1073 (1996).

- [5] C. Zalka, Proc. R. Soc. London A **454**, 313 (1998).
- [6] J. Preskill, Quantum **2**, 79 (2018).
- [7] For a recent review on superconducting qubits, see G. Wendin, Rep. Prog. Phys. **80**, 106001 (2017).
- [8] For a recent review of trapped-ion based platforms, see, e.g., C. D. Bruzewicz, J. Chiaverini, R. McConnell, and J. M. Sage, Appl. Phys. Rev. **6**, 021314 (2019).
- [9] For an up-to-date review of Rydberg-atom based platforms, see, e.g., M. Morgado and S. Whitlock, AVS Quantum Sci. **3**, 023501 (2021).
- [10] D. S. Abrams and S. Lloyd, Phys. Rev. Lett. **79**, 2586 (1997); *ibid.* **83**, 5162 (1999).
- [11] R. Somma, G. Ortiz, J. E. Gubernatis, E. Knill, and R. Laflamme, Phys. Rev. A **65**, 042323 (2002).
- [12] S. B. Bravyi and A. Y. Kitaev, Ann. Phys. (N.Y.) **298**, 10 (2002).
- [13] See, e.g., J. D. Whitfield, I. Biamonte, and A. Aspuru-Guzik, Mol. Phys. **109**, 735 (2011).
- [14] S. Raesi, N. Wiebe, and B. C. Sanders, New J. Phys. **14**, 103017 (2012).
- [15] D. Wecker, M. B. Hastings, N. Wiebe, B. K. Clark, C. Nayak, and M. Troyer, Phys. Rev. A **92**, 062318 (2015).
- [16] R. Barends, L. Lamata, J. Kelly, L. García-Álvarez, A. G. Fowler, A. Megrant, E. Jeffrey, T. C. White, D. Sank, J. Y. Mutus, *et al*, Nat. Commun. **6**, 7654 (2015).
- [17] R. Babbush, N. Wiebe, J. McClean, J. McClain, H. Neven, and G. K. Chan, Phys. Rev. X **8**, 011044 (2018).
- [18] J.-M. Reiner, S. Zanker, I. Schwenk, J. Leppäkangas, F. Wilhelm-Mauch, G. Schön, and M. Marthaler, Quantum Sci. Technol. **3**, 045008 (2018).
- [19] Z. Jiang, K. J. Sung, K. Kechedzhi, V. N. Smelyanskiy, and S. Boixo, Phys. Rev. Appl. **9**, 044036 (2018).
- [20] N. C. Rubin, T. Shiozaki, K. Throssell, G. K. Chan, and R. Babbush, arXiv:2104.13944.
- [21] For a recent review of applications in quantum chemistry, see, e.g., S. McArdle, S. Endo, A. Aspuru-Guzik, S. C. Benjamin, and X. Yuan, Rev. Mod. Phys. **92**, 015003 (2020).
- [22] A. Mezzacapo, J. Casanova, L. Lamata, and E. Solano, Phys. Rev. Lett. **109**, 200501 (2012).
- [23] A. Macridin, P. Spentzouris, J. Amundson, and R. Harnik, Phys. Rev. Lett. **121**, 110504 (2018).
- [24] A. Macridin, A. C. Y. Li, S. Mrenna, and P. Spentzouris, Phys. Rev. A **105**, 052405 (2022).
- [25] A. Di Paolo, P. Kl. Barkoutsos, I. Tavernelli, and A. Blais, Phys. Rev. Research **2**, 033364 (2020).
- [26] N. Fitzpatrick, H. Apel, and D. Muñoz Ramo, arXiv:2106.03985.
- [27] A. Miessen, P. J. Ollitrault, and I. Tavernelli, Phys. Rev. Research **3**, 043212 (2021).
- [28] For a recent review, see F. Giustino, Rev. Mod. Phys. **89**, 015003 (2017).
- [29] T. Holstein, Ann. Phys. (N.Y.) **8**, 343 (1959).
- [30] G. Wellein and H. Fehske, Phys. Rev. B **56**, 4513 (1997).
- [31] For an introduction, see D. Emin, Phys. Today **35**, 34 (1982), and references therein.
- [32] K. Hannewald, V. M. Stojanović, and P. A. Bobbert, J. Phys.: Condens. Matter **16**, 2023 (2004).
- [33] V. M. Stojanović, P. A. Bobbert, and M. A. J. Michels, Phys. Rev. B **69**, 144302 (2004).
- [34] E. I. Shneyder, S. V. Nikolaev, M. V. Zotova, R. A. Kaldin, and S. G. Ovchinnikov, Phys. Rev. B **101**, 235114 (2020).
- [35] V. M. Stojanović, N. Vukmirović, and C. Bruder, Phys. Rev. B **82**, 165410 (2010).
- [36] V. M. Stojanović and M. Vanević, Phys. Rev. B **78**, 214301 (2008).
- [37] J. Sous, M. Chakraborty, C. P. J. Adolphs, R. V. Krems, and M. Berciu, Sci. Rep. **7**, 1169 (2017).
- [38] V. M. Stojanović, M. Vanević, E. Demler, and L. Tian, Phys. Rev. B **89**, 144508 (2014).
- [39] V. M. Stojanović, Phys. Rev. B **101**, 134301 (2020).
- [40] V. M. Stojanović, T. Shi, C. Bruder, and J. I. Cirac, Phys. Rev. Lett. **109**, 250501 (2012).
- [41] F. Herrera, K. W. Madison, R. V. Krems, and M. Berciu, Phys. Rev. Lett. **110**, 223002 (2013).
- [42] F. Mei, V. M. Stojanović, I. Siddiqi, and L. Tian, Phys. Rev. B **88**, 224502 (2013).
- [43] V. M. Stojanović and I. Salom, Phys. Rev. B **99**, 134308 (2019).
- [44] J. K. Nauth and V. M. Stojanović, Phys. Rev. B **107**, 174306 (2023).
- [45] B. Jaderberg, A. Eisfeld, D. Jaksch, and S. Mostame, New J. Phys. **24**, 093017 (2022).
- [46] C. Slezak, A. Macridin, G. A. Sawatzky, M. Jarrell, and T. A. Maier, Phys. Rev. B **73**, 205122 (2006).
- [47] L.-C. Ku and S. A. Trugman, Phys. Rev. B **75**, 014307 (2007).
- [48] H. Fehske, G. Wellein, and A. R. Bishop, Phys. Rev. B **83**, 075104 (2011).
- [49] S. Tomimoto, H. Nansei, S. Saito, T. Suemoto, J. Takeda, and S. Kurita, Phys. Rev. Lett. **81**, 417 (1998); S. L. Dexeheimer, A. D. Van Pelt, J. A. Brozik, and B. I. Swanson, *ibid.* **84**, 4425 (2000); A. Sugita, T. Saito, H. Kano, M. Yamashita, and T. Kobayashi, *ibid.* **86**, 2158 (2001).
- [50] H. F. Trotter, Proc. Am. Math. Soc. **10**, 545 (1959).
- [51] M. Suzuki, Commun. Math. Phys. **51**, 183 (1976).
- [52] P. Jordan and E. Wigner, Z. Phys. **47**, 631 (1928).
- [53] V. M. Stojanović, Phys. Rev. Lett. **124**, 190504 (2020).
- [54] V. M. Stojanović, Phys. Rev. A **103**, 022410 (2021).
- [55] C. Schön, K. Hammerer, M. M. Wolf, J. I. Cirac, and E. Solano, Phys. Rev. A **75**, 032311 (2007).
- [56] M. A. Nielsen and I. L. Chuang, *Quantum Computation and Quantum Information* (Cambridge University Press, Cambridge, 2000).
- [57] R. Cleve, A. Ekert, C. Macchiavello, and M. Mosca, Proc. R. Soc. London. Ser. A Math. Phys. Eng. Sci. **454**, 339 (1998).
- [58] M. Heyl, Rep. Prog. Phys. **81**, 054001 (2018).
- [59] A. Peres, Phys. Rev. A **30**, 1610 (1984).
- [60] J. K. Cullum and R. A. Willoughby, *Lanczos Algorithms for Large Symmetric Eigenvalue Computations* (Birkhäuser, Boston, 1985).
- [61] H. Tal-Ezer and R. Kosloff, J. Chem. Phys. **81**, 3967 (1984).
- [62] R. Kosloff, Annu. Rev. Phys. Chem. **45**, 145 (1994).
- [63] See, e.g., J. Jager and R. Barnett, Phys. Rev. Research **3**, 033212 (2021).
- [64] For a review, see A. Mitra, Annu. Rev. Condens. Matter Phys. **9**, 245 (2018).
- [65] A. Smith, M. S. Kim, F. Pollmann, and J. Knolle, npj Quantum Inf. **5**, 106 (2019).
- [66] A. M. Childs, D. Maslov, Y. Nam, N. J. Ross, and Y. Su, Proc. Natl. Acad. Sci. USA **115**, 9456 (2018).
- [67] A. Bolens and M. Heyl, Phys. Rev. Lett. **127**, 110502 (2021).
- [68] M. Geller, Z. Holmes, P. J. Coles, and A. Sornborger,

